Inorganic Chemistry

Communication

pubs.acs.org/IC

Quaternary Supertetrahedra-Layered Telluride $CsMnInTe_3$: Why Does This Type of Chalcogenide Tilt?

Hua Lin,[†] Jin-Ni Shen,[†,‡] Ling Chen,[†] and Li-Ming Wu*[,†]

[†]State Key Laboratory of Structural Chemistry, Fujian Institute of Research on the Structure of Matter, Chinese Academy of Sciences, Fuzhou, Fujian 350002, People's Republic of China

[‡]University of Chinese Academy of Sciences, Beijing 100039, People's Republic of China

Supporting Information

ABSTRACT: Dark-red $CsMnInTe_3$ is synthesized by a solid-state approach using CsCl as the reactive flux. This layered compound is constructed by T_3 supertetrahedra and crystallizes in the space group $C2/c$ with a = 12.400(7) Å, b = 12.400(7) Å, c = 24.32(2) Å, β = 97.31(2)°, and V = 927.07(6) Å^3. The electrostatic interactions cause tilting of the supertetrahedra layers, and the value of the tilting angle is fixed by a structure index, $\beta' = 180° - \arccos(a/4c)$. Such an index is valid for all of the members in this family known to date.

Semiconducting chalcogenides have attracted considerable interest in chemistry and materials science because of their rich structural chemistry and diverse physical properties, such as thermoelectric,[1] nonlinear-optical,[2] photoluminescent,[3] and photocatalytic properties.[4] Among them, compounds constructed by supertetrahedral clusters (denoted as T_n, n = 2, 3), i.e., $CsHgInS_3$[5] and $CsCdInTe_3$,[6] show remarkable photoconductive properties and are considered as promising candidates for hard X-ray and γ-ray radiation detection. Generally, most of the known supertetrahedra compounds are inorganic−organic hybrids,[7] pure inorganic supertetrahedra-layered compounds are comparatively less reported, and only 25 sulfides and selenides and 5 tellurides are known.[8] All of the known supertetrahedra-layered compounds are monoclinic! This caught our attention: why do supertetrahedra-layered compounds inevitably crystallize in the monoclinic system? However, this has never been explored. In this Communication, a new layered telluride member, $CsMnInTe_3$ (**1**), constructed by T_3 supertetrahedra has been discovered. Interestingly, we find that the tilting of each T_3 layer along the packing direction is fixed by a tilting index β'. More interestingly, such an index well predicts within 0.5% deviation the tilting of all 31 compounds known to date including ternary and quaternary compounds with different compositions and stoichiometries. Besides, the syntheses, structures as well as magnetic property, and electronic structures of **1** are reported.

Layered **1** was synthesized by a facile solid-state approach using CsCl as the reactive flux and loading ratios of CsCl/Mn/In/Te = x/3/2/6 (x = 3, 5). The yield is 85% based on In (Supproting Information, SI) Compound **1** is isostructural to $Rb_2Cu_2Sn_2S_6$[9] and crystallizes as dark-red plates in the space group $C2/c$ (No. 15).[10] As shown in Figure 1a,c, the building units are $[Mn_4In_6Te_{20}]^{14-}$ supertetrahedra (T_3) that are condensed into $[Mn_2In_2Te_6]^{2-}$ layers. These layers are packed into an ABA pattern along the c axis. Such a structure is conceptually related to a ternary $CsInTe_2$ (**2**) by removing 1 equiv of a MnTe sheet from the $[Mn_2In_2Te_6]^{2-}$ layer (Figure 1) similar to that found in $CsCdInTe_3$.[6] During composition of this paper, **2** was reported by the Kanatzidis group by a different polychalcogenide flux method.[6] Here, **2** (dark-red irregular plates) was synthesized by a totally different method, indicated by the reaction of 6CsCl + La + 3In + 6Te → 3$CsInTe_2$ + Cs_3LaCl_6 with a loading ratio of CsCl/La/In/Te = 10/1/3/6 (the yield is 100% based on In). Excess CsCl and byproduct Cs_3LaCl_6 were washed off by distilled water (SI). Compound **2** also crystallizes in $C2/c$ (Table S1 in the SI).[11] **1** is stable in air for several days, but **2** is air-sensitive and the crystal surface turns black within a few hours.

In the structure of **1** (Figure 1a), each of the two crystallographically independent Cs atoms is 8-fold-coordinated to Te^{2-} anions in a bicapped trigonal prism with Cs−Te distances ranging from 3.812(2) to 4.429(2) Å that are comparable to those in **2** (Tables S4 and S5 in the SI). These are consistent with those in $CsTi_5Te_8$ (3.791−3.994 Å),[12] $Cs_2Mn_3Te_4$ (3.887−3.947 Å),[13] and CsY_2CuTe_4 (3.686−4.283 Å).[14] Figure S5 in the SI shows that Cs^+ cations locate at the grooves of each $[Mn_2In_2Te_6]^{2-}$ layer via electrostatic attraction. Such a layer is built by primitive $[InTe_4]$ and $[MnTe_4]$ tetrahedra with normal In−Te or Mn−Te distance (Table S5 in the SI). The $[InTe_4]$ and $[MnTe_4]$ tetrahedra form a $[Mn_4In_6Te_{20}]^{14-}$ supertetrahedra (T_3) via sharing vertexes (Figure 1c). Further, these T_3 supertetrahedra fuse into the anionic $[Mn_2In_2Te_6]^{2-}$ layer via sharing common corners (Figure 1a,c). Interestingly, such a T_3 supertetrahedra can be conceptually reduced to a $[In_4Te_{10}]^{8-}$ supertetrahedra (T_2) in **2** by removing four $[MnTe_4]$ tetrahedra (Figure 1d) without breaking the overall symmetry. Consequently, both **1** and **2** crystallize in $C2/c$ with similar a, b, and β values and only differ in the c values, which decrease from 24.32(2) Å in **1** to 18.11(2) Å in **2** because of the decrease of the layer thickness by removal of the MnTe layer (Figure 1).

Because there are two or more ways for the neighboring $[Mn_2In_2Te_6]^{2-}$ layers in **1** to stack with respect to one another, why do these layers only pack into the monoclinic symmetry? The same is true for **2**. For clarity, let us look at an abstract (010) view of **1** and **2**, as shown in Figure 1e, in which the rectangle represents the anionic layer. Keep in mind that between the

Received: July 18, 2013
Published: September 19, 2013

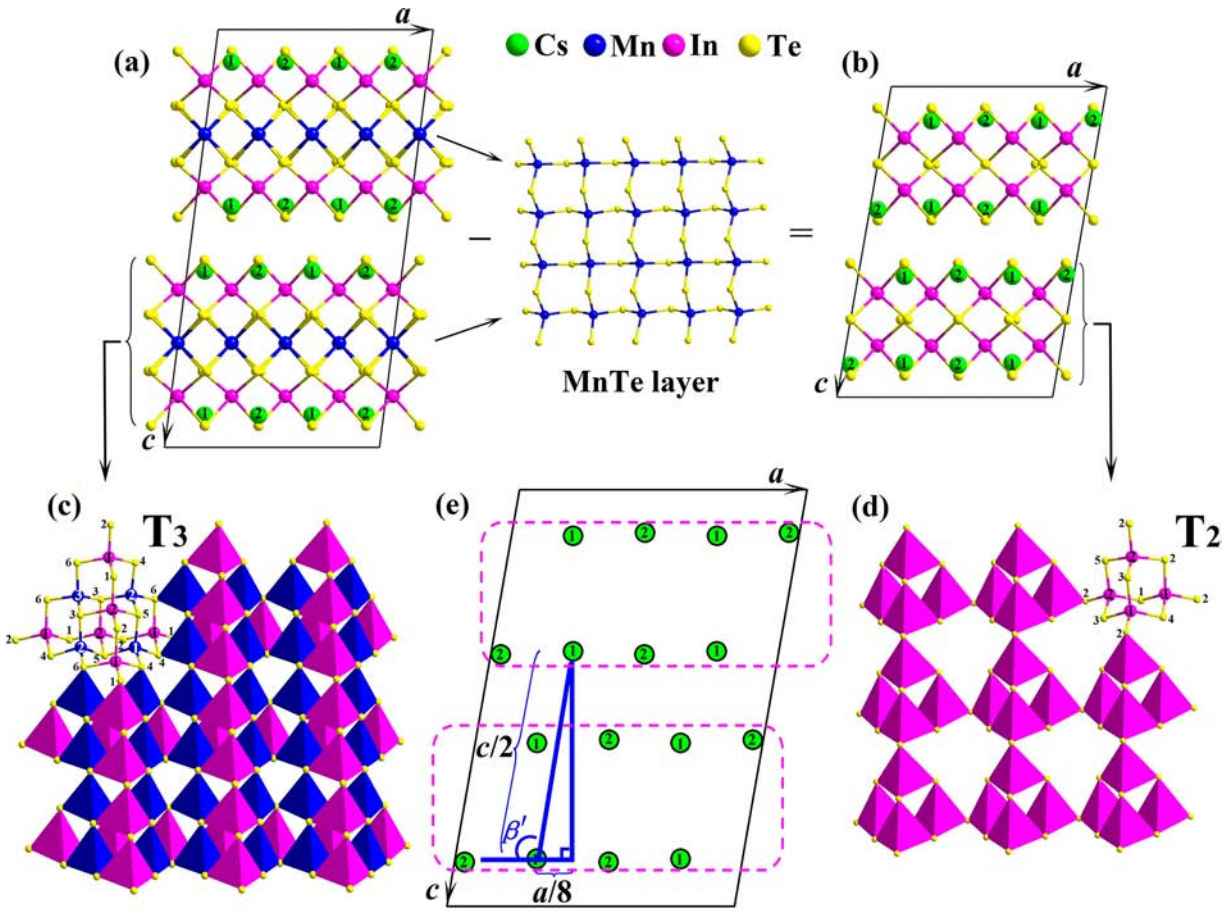

Figure 1. (010) structure views of (a) **1** and (b) **2** with unit cells marked. (c) Single T_3 layer in **1** with the $[Mn_4In_6Te_{20}]^{14-}$ supertetrahedra (T_3) outlined and with atom numbers marked. (d) Single T_2 layer in **2** with the $[In_4Te_{10}]^{8-}$ supertetrahedra (T_2) outlined and with atom numbers marked. (e) Abstract (010) view of the structures of **1** and **2** with the anionic layer simplified as a rectangle. The definition of the tilting index β' and projections of Cs^+ cations within a unit cell are marked.

layers there are no covalent or metallic bonding interactions, and thus the electrostatic interactions (namely, the Cs−Te ionic bonding interactions) are dominant. Naturally, during packing, the Cs1 cation on the upper layer tries to minimize the electrostatic repulsion from the cations on the lower layer, and as a result, the only geometric and energetic stable position for Cs1 has to be at the perpendicular bisector of the line between the nearest Cs1 and Cs2 cations on the neighboring lower layer. Similar is true for the Te anions. Consequently, the upper layer shifts along the a axis with respect to the lower layer. This answers why the layers are tilted.

Also, the next questions are, how much is the tilting and can we predict it? As shown in Figure 1e, on the lower layer, if l is the distance between Cs1 and Cs2 projected along the a axis, because there are four such l values per unit cell, then l equals $a/4$. Together with the above discussion, the length of the short cathetus of the blue right-angled triangle shown in Figure 1e is deduced to be $8/a$. Also, the length of the hypotenuse equals $2/c$ because there are two layers per unit cell. Then we obtain the value of the β' angle by the equation $\beta' = 180° - \arccos(a/4c)$. For **1**, β' is calculated to be 97.32°, agreeing very well with the crystallographic β angle [97.31(2)°; Table S1 in the SI]. For **2**, β' = 99.83° is also in good agreement with β [99.891(1)°]. More significantly, for all of the available 30 other compounds, the calculated β' values equal to the experimental β angles within 0.5% deviation (Table S5 in the SI). Consequently, we define β' as a structure index to indicate the tilting of the layer.

Besides, we have also studied the magnetic properties of **1**. As shown in Figure 2a, the susceptibility obeys the Curie−Weiss law

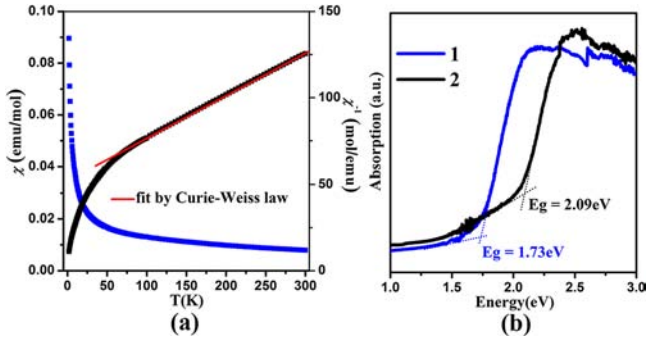

Figure 2. (a) Temperature dependence of the molar magnetic susceptibility (χ; blue) and the inverse molar magnetic susceptibility (χ^{-1}; black) of **1**. (b) UV−vis diffusion reflectance spectra of **1** and **2**.

above 55 K with C = 4.27 emu·K/mol and θ = −216.32 K. The calculated effective magnetic moment ($\mu_{eff} \approx 5.85\ \mu_B$/Mn) according to the equation $\mu_{eff} = (7.997C)^{1/2}\mu_B$ [15] deviates slightly from the theoretical value for a high-spin Mn^{2+} (5.92 μ_B/Mn). The large negative θ suggests significant antiferromagnetic interactions between the Mn^{2+} cations (the nearest Mn−Mn distance is 4.31 Å).

dx.doi.org/10.1021/ic4018618 | Inorg. Chem. 2013, 52, 10726−10728

To understand such magnetic interactions in **1**, we have calculated three different models, i.e., nonmagnetic (NM), ferromagnetic (FM), and antiferromagnetic (AFM) models (Figure S7 in the SI). As listed in Table S6 in the SI, the total energies of the FM and AFM models are lower than that of the NM model. Also, the AFM-1 model is the most stable configuration, which is about 20 and 1 eV lower than those of the NM and FM models, respectively. These results support the AFM interaction observations in **1**. The band structure studies reveal that both compounds **1** and **2** are direct semiconductors (Figure S6 in the SI). The calculated band gaps E_g(cal), 1.27 and 1.35 eV, show the same increasing trend on going from **1** to **2** as the experimental results [E_g(obs) = 1.73 eV for **1** and 2.09 eV for **2**; Figure 2b]. As shown in Figure 3, the total and partial densities

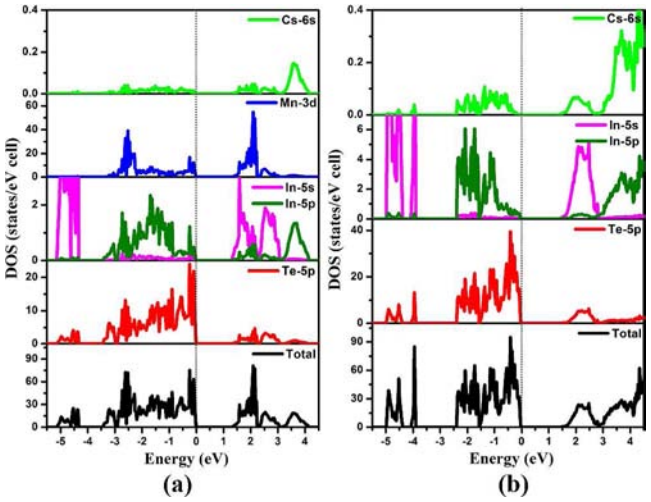

Figure 3. Total and partial DOSs of (a) **1** and (b) **2**.

of states (DOSs) of **1** and **2** are similar. The Cs atoms almost make no contribution around E_F and act as electron donors to stabilize the structure. Mn atoms contribute around E_F at the top of the valence band and the bottom of the conduction band, whereas Te 5p states contribute mostly near E_F. Thus, the band gap of **1** is determined by the electron transition from Te 5p and Mn 3d to Mn 3d, Te 5p, In 5s, and In 5p. As a result, inserting Mn into **2** decreases the band gap. This helps one to understand the observations shown in Figure 2b. Figure 3 also indicates that taking out Mn states from **1** ($CsMnInTe_3$, 2D layered) to "generate" **2** ($CsInTe_2$, 2D layered) does not change the dimensionality, but the thickness of the layer has been decreased, and the band gap increases. This should be a supplement to the concept of the "dimensional reduction" of chalcogenides.[16]

In summary, a new quaternary layered telluride **1** has been synthesized by a facile approach by using CsCl as the reactive flux. Compound **1** is constructed of T_3 clusters. The VASP calculations reveal its semiconducting feature, which agrees, in principle, with experimental observation. The magnetic property studies suggest that the AFM interactions between Mn^{2+} centers adopting high-spin configurations are the energetic favorite. The structure relationship between **1** and ternary **2** is discussed. For the first time, we point out that the packings of all of the supertetrahedra-layered chalcogenides known to date are tilting because of electrostatic interactions. Also, the tilting angles are fixed by the structure index β' [$\beta' = 180° - \arccos(a/4c)$]. Further exploration into the correlations between the β' index and the size/distortion of the MTe_4 building unit, the property of the compound, etc., would be very interesting. Such a general structural relationship would shed some useful light on the structure understanding and the prediction/design of new compounds.

■ ASSOCIATED CONTENT

Ⓢ Supporting Information

CIF data, experimental and theoretical methods, and additional tables and figures. This material is available free of charge via the Internet at http://pubs.acs.org.

■ AUTHOR INFORMATION

Corresponding Author

*E-mail: liming_wu@fjirsm.ac.cn. Tel: (011)86-591-83705401.

Notes

The authors declare no competing financial interest.

■ ACKNOWLEDGMENTS

This research was supported by the National Natural Science Foundation of China under Projects 20973175, 21171168, 21225104, and 21233009.

■ REFERENCES

(1) (a) Chung, D. Y.; Hogan, T.; Brazis, P.; Rocci-Lane, M.; Kannewurf, C.; Bastea, M.; Uher, C.; Kanatzidis, M. G. *Science* **2000**, *287*, 1024. (b) Hsu, K. F.; Loo, S.; Guo, F.; Chen, W.; Dyck, J. S.; Uher, C.; Hogan, T.; Polychroniadis, E. K.; Kanatzidis, M. G. *Science* **2004**, *303*, 818.

(2) (a) Chung, I.; Jang, J. I.; Malliakas, C. D.; Ketterson, J. B.; Kanatzidis, M. G. *J. Am. Chem. Soc.* **2010**, *132*, 384. (b) Yu, P.; Zhou, L. J.; Chen, L. *J. Am. Chem. Soc.* **2012**, *134*, 2227.

(3) (a) Banerjee, S.; Malliakas, C. D.; Jang, J. I.; Ketterson, J. B.; Kanatzidis, M. G. *J. Am. Chem. Soc.* **2008**, *130*, 12270. (b) Banerjee, S.; Szarko, J. M.; Yuhas, B. D.; Malliakas, C. D.; Chen, L. X.; Kanatzidis, M. G. *J. Am. Chem. Soc.* **2010**, *132*, 5348.

(4) (a) Lei, Z.; You, W.; Liu, M.; Zhou, G.; Takata, T.; Hara, M.; Domen, K.; Li, C. *Chem. Commun.* **2003**, *17*, 2142. (b) Chen, D.; Ye, J. H. *J. Phys. Chem. Solids* **2007**, *68*, 2317.

(5) Li, H.; Malliakas, C. D.; Liu, Z.; Peters, J. A.; Jin, H.; Morris, C. D.; Zhao, L.; Wessels, B. W.; Freeman, A. J.; Kanatzidis, M. G. *Chem. Mater.* **2012**, *24*, 4434.

(6) Li, H.; Malliakas, C. D.; Peters, J. A.; Liu, Z.; Im, J.; Jin, H.; Morris, C. D.; Zhao, L.; Wessels, B. W.; Freeman, A. J.; Kanatzidis, M. G. *Chem. Mater.* **2013**, *25*, 2089.

(7) (a) Li, H.; Laine, A.; O'Keeffe, M.; Yaghi, O. M. *Science* **1999**, *283*, 1145. (b) Zheng, N.; Bu, X.; Wang, B.; Feng, P. *Science* **2002**, *298*, 2366. (c) Dehnen, S.; Melullis, M. *Coord. Chem. Rev.* **2007**, *251*, 1259.

(8) Listed in Table S6 (SI) and 19 references therein.

(9) Liao, J. H.; Kanatzidis, M. G. *Chem. Mater.* **1993**, *5*, 1561.

(10) X-ray crystal data for **1** at 293(2) K: monoclinic; *C*2/*c*; *Z* = 16; *a* = 12.395(7) Å, *b* = 12.400(7) Å, *c* = 24.32(2) Å, β = 97.31(2)°.

(11) X-ray crystal data for **2** at 293(2) K: monoclinic; *C*2/*c*; *Z* = 16; *a* = 12.355(7) Å, *b* = 12.362(7) Å, *c* = 18.11(2) Å, β = 99.891(6)°.

(12) Gray, D. L.; Ibers, J. A. *J. Alloys Compd.* **2007**, *440*, 74.

(13) Bronger, W.; Hardtdegen, H.; Kanert, M.; Mueller, P.; Schmitz, D. *Z. Anorg. Allg. Chem.* **1996**, *622*, 313.

(14) Babo, J. M.; Schleid, T. *Solid State Sci.* **2010**, *12*, 238.

(15) O'Connor, C. *J. Prog. Inorg. Chem.* **1982**, *29*, 209.

(16) (a) Axtell, E. A.; Park, Y.; Chondroudis, K.; Kanatzidis, M. G. *J. Am. Chem. Soc.* **1998**, *120*, 124. (b) Androulakis, J.; Peter, S. C.; Li, H.; Malliakas, C. D.; Peters, J. A.; Liu, Z. F.; Wessels, B. W.; Song, J. H.; Jin, H.; Freeman, A. J.; Kanatzidis, M. G. *Adv. Mater.* **2011**, *23*, 4163.